Compensation of emulated atmospheric disturbance and tracking of a moving object by a real-time digital phase conjugate mirror using a liquid crystal spatial light modulator

Engineering Research Express

PAPER

Compensation of emulated atmospheric disturbance and tracking of a moving object by a real-time digital phase conjugate mirror using a liquid crystal spatial light modulator

RECEIVED
8 March 2023

REVISED
4 May 2023

ACCEPTED FOR PUBLICATION
12 May 2023

PUBLISHED
30 May 2023

Kotomi Kawakami[1], **Tomoya Nakagawa**[2], **Hiroto Tanaka**[2] and **Hideki Okamura**[2]

[1] Physics Section, Center for Natural Sciences, College of Liberal Arts and Sciences, Kitasato University, Kanagawa, 252-0373, Japan
[2] Department of Physics, Graduate School of Natural Sciences, International Christian University, Tokyo, 181-8585, Japan

E-mail: k-kawa@kitasato-u.ac.jp

Keywords: digital optical phase conjugation, wireless optical transfer, atmospheric disturbance correction, wavefront compensation

Abstract

We developed a fast-response digital phase conjugate mirror using a 700 Hz high-speed liquid crystal spatial light modulator and a high-speed camera. The total delay from signal light acquisition to phase conjugate light generation was 9.7 ms at 1246 × 1024 and 5.9 ms at 640 × 512. The tracking experiment performed on a target moving at a constant distance perpendicular to the optical axis, produced an error of 2%. Furthermore, a heated soldering iron, used to compensate for artificially generated air disturbance, showed that beam wandering and intensity fluctuations were reduced by 86% and 55%, respectively, compared to a phase conjugate mirror with added delay. Phase conjugate light irradiation of a continuously moving target at a maximum speed of 0.9 mm s^{-1} was also performed. This study shows that real-time digital phase conjugate mirrors can correct wavefront distortion caused by air fluctuation, which is a major challenge in long-distance wireless optical transmission in the turbulent atmosphere, without complicated control, and prevent beam quality degradation in the presence of atmospheric disturbance.

Introduction

In recent years, wireless optical transmission in the atmosphere has been rapidly gaining attention among researchers in the field of optics. In addition to civilian applications, such as long-distance free-space wireless optical communications between ground and satellites, these wireless optical transmissions have potential applications in space development, including wireless power supply for flying objects such as drones and space solar power generation [1, 2].

However, turbulence-induced fluctuations in the refractive index of air can distort the wavefront of light beams traveling in the atmosphere, causing beam wandering, scintillation, and diffusion of the optical beam [3–5].

In general, gimbal mirrors comprise the most commonly used method for the irradiation of remote targets with light [6, 7]. This method, in which a motor is used to rotate and steer the mirror, is highly ineffective in terms of compensating distortions in light wavefronts caused by atmospheric disturbances. Although adaptive optics (AO) for wireless optical transmission has been extensively studied, AO requires complex control of a wavefront sensor and a variable mirror whose number of controllable modes remains limited because the number of actuators for a variable mirror can only be a few hundred at most [8–10].

The phase conjugate mirror generates light with identical wavefronts as the incident light in the opposite direction without mechanical control [11]. Since the replica of the incident light, or phase conjugate light, retraces the original incident light path, it automatically travels back to the light source. In addition, optical wavefront distortions are canceled when the phase conjugate light travels backward along the same path [12]. Consequently, the original beam quality can be restored, enabling light to be irradiated close to the diffraction limit. Therefore, irradiation of a large space using the probe light enables the phase conjugate light to

automatically capture, track, and focus the light beam on a moving object based on the signal reflected from the target even in the presence of atmospheric disturbances.

Conventional generation methods of phase conjugate light use nonlinear optical media. However, each medium used has one or more difficulties, including wavelength limitations, threshold of incident light intensity, and narrow aperture, but also frequency shift, different response time, and energy misbalance with the incident light [13, 14]. In contrast, we have adopted a digital method for generating phase conjugate light that uses a camera and a spatial light modulator [15, 16]. In this digital method, the camera records the incident light, and the spatial light modulator then generates the phase conjugate light in a way that recording and playback are performed at different locations. Consequently, this eliminates unnecessary interactions between the light beams and allows for a highly versatile device with no intensity or frequency limitations. For example, our method enables the acquisition of target information at wavelengths with low scattering characteristics and the emission of phase conjugate light at wavelengths with high absorption at the target, including the acquisition of data from the object when necessary. In particular, the use of digital devices facilitates larger sizes, and the large aperture facilitates long-distance wireless optical transmission using high intensity lasers.

Digital phase conjugate mirrors have often used liquid crystal spatial light modulators (SLM) [17]. They are used in various field such as beam steering, beam shaping for laser processing and optical sensing. Liquid crystal SLM have the advantages of high fidelity due to grayscale modulation and simple setup. However, the delay imposed by the orientation time of the liquid crystal molecules is significantly high [18]. For instance, a previous study reported that the total delay between the acquisition of images and the generation of phase conjugate light was approximately 0.1 s [19]. In order to generate phase conjugate light before atmospheric conditions change, response time of the digital phase conjugate mirror should be short. The velocity of atmospheric turbulence fluctuations is expressed as the time $\tau = r_0/v$ in which the turbulent velocity (wind speed) v passes through the Fried (coherence) length r_0, the length at which the wavefront can be considered a plane wave. For example, Sergeyev *et al* measured Fried lengths from 2 mm to 15 cm over a path of more than 3 km at an elevation of 250 m [20]. Assuming a wind speed of 10 m s^{-1}, the fluctuation time ranges from 0.2 to 15 ms. Therefore, a response time of the order of milliseconds or less is required to freeze the fluctuations of atmospheric turbulence. Wang *et al* obtained a response time of 5.3 ms at 1920 × 1080 using a microoptoelectromechanical system based on a digital mirror device (DMD) and field-programmable gate array (FPGA) instead of a liquid crystal modulator [21]. However, DMD can only perform binary modulation and must be an off-axis system.

In this study, we improved the real-time performance of this system using a 700 Hz high-speed liquid crystal SLM and a high-speed camera. High-speed SLM can stabilize liquid crystal molecules in 1.4 ms using the overdrive technique, which fulfils the application of this study. In our system, the photographed interference fringes are directly displayed on the SLM and the light is diffracted to generate phase conjugate light. Therefore, there are no mechanical drive components and no need for phase retrieval, which is performed by phase-modulated-type digital phase conjugation, so the speed can be increased. We achieved total delay times of 9.7 ms and 5.9 ms at 1246 × 1024 and 640 × 512, respectively, and demonstrated tracking of a moving target and real-time wavefront compensation in artificial atmospheric disturbance.

Experiments and results

As shown in figure 1, the device records and reproduces optical information from a target using two lasers. Instead of a nonlinear optical medium, a charge coupled device (CCD) camera is used to record interference fringes created by the target signal beam, which are transferred to a liquid crystal SLM and retrieved by the other laser. In this study, images from a high-speed streaming camera (Infinicam UC-1), with 1246 × 1024 resolution and maximum 1000 fps image capture speed, are transferred to a 1920 × 1152 high-speed liquid crystal on silicon (LCOS) type SLM (meadowlark optics) driven at 714 Hz (table 1). The difference in pixel size between the camera and the SLM is compensated by placing a lens system in front of Camera 1. The captured interference fringe patterns are sent to a PC via USB 3.1 and displayed on a high-speed SLM via PCIe. A frequency stabilized He-Ne laser was used for recording interference fringes, and a He-Ne laser was used for reading out. The light from Laser1 (recording) is made into a Michelson interferometer using PBS1. One arm is directed to a spherical mirror with f = −200 as a probe light for target detection, and the reflected light is incident on Camera 1 as a signal light from a virtual point source. The other arm is reflected by the mirror and is vertically incident on Camera 1, and interferes with the reference light to produce interference fringes. Though the coherence length becomes an issue, reference light can be created by bifurcating and filtering the signal light with zero-path length difference [22]. The image of the interference fringes is displayed on SLM, and when the light from Laser 2 is directed perpendicularly to the SLM, a part of the light becomes phase conjugate light through diffraction. Since the optical paths of the signal light from the target and the generated phase conjugate light are decoupled by PBS 2, Camera 1 and SLM need to be placed at the same position optically across PBS 2. Part of the phase conjugate

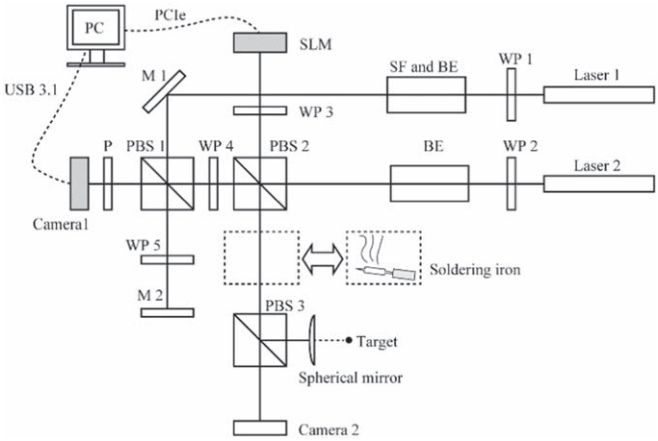

Figure 1. A schematic diagram of the experimental setup. Two He-Ne lasers (Lasers 1 and 2) are used to record and playback, respectively. WP 1 and 2 are half-wave plates, while WP 3–5 are quarter-wave plates. SF: spatial filter, BE: beam expander, PBS: polarizing beam splitter, M: mirror, and P: polarizer. Cameras 1 and 2 are used for fringe recording and observation, respectively. The spherical mirror is placed on a rail for tracking tests, and a soldering iron is placed under the light path surrounded by dotted lines during correction tests for artificial air disturbances.

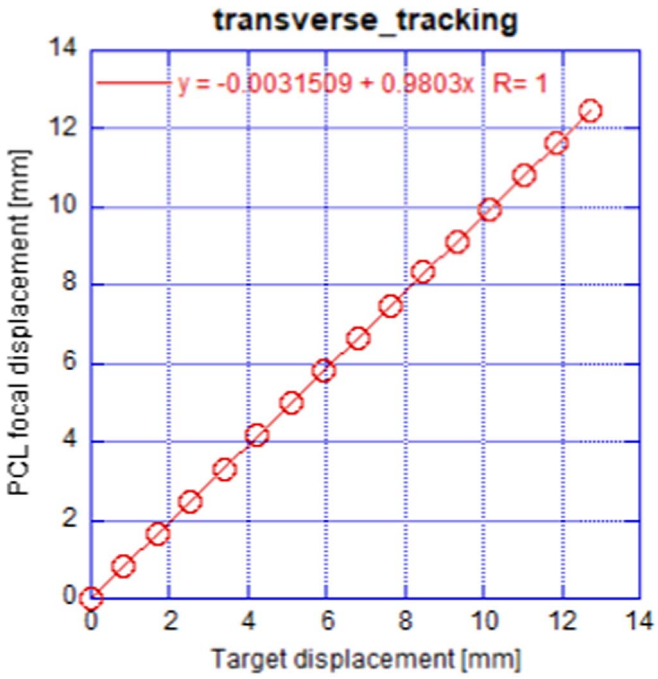

Figure 2. Movement of the phase conjugate light when the virtual point light source was moved.

light generated by SLM enters the observation arm at PBS 3, while the other part is focused 200 mm behind the spherical mirror. In this experiment, the size of the phase conjugate light focus was 1.1 times the diffraction limit.

The first step was to measure the response speed. The response time was measured using a Photron AXmini high-speed camera. A mechanical shutter was used to turn off and on the light of Laser 1, and the timing of the appearance and disappearance of the phase conjugate light was measured in relation to the blinking of the light of Laser 1. Our results showed that the response times were 9.7 ± 1.7 ms for the 1246×1024 pixel INIFINICAM UC-1 and 5.9 ± 2.3 ms for the 640×512 downsampled XIMEA MQ013MG, which were comparable to the response time reported in Wang *et al* [20].

Next, we performed our tracking experiment. The target position was moved in the direction perpendicular to the optical axis at constant intervals, and the focal position of the phase conjugate light was monitored. Our findings revealed that the phase conjugate light moved exactly the same distance as the spherical mirror (figure 2), indicating that it followed the movement of the target with an error of 2%.

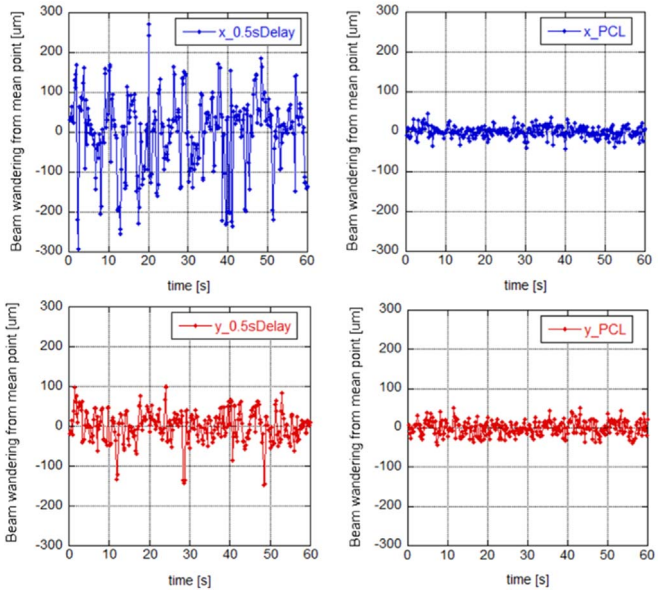

Figure 3. Wavefront compensation experiment. Beam wandering was measured with phase conjugate light generated with a delay of 0.5 sec (left) and in real time (right). Angular fluctuations are reduced by 86% in the x-direction (top) and 53% in the y-direction (bottom).

Table 1. Specifications of experimental apparatus.

Optical digital phase conjugate mirror characteristics		
He-Ne laser output power	1	mW
Sperical mirror	−200	mm
Soldering iron	100	W
PCL output	tens of nW	
Infinicam UC-1 (photoron)		
resolution	1246 × 1024	pixel
pixel size	10	μm
frame per sec (max.)	988	fps
MQ013MG-ON (Ximea)		
resolution	1280 × 1024	pixel
pixel size	5	μm
frame per sec (max.)	210	fps
SLM (HSP1920–500–1200-HSP8 CX (Meadowalk optics)		
resolution	1920 × 1152	pixel
pixel pitch	9	μm
system frame rate	714	Hz

Next, a 100-W soldering iron was placed under the optical path to emulate randum intensity and phase fluctuations to test the wavefront distortion compensation effect of the phase conjugate light in dynamic air disturbance [23]. The wandering of the center of the beam at Camera 2 was assessed with phase conjugate light that was delayed by 0.5 s. When the 0.5-s delay was added, the state of disturbance changed before the phase conjugate light could be generated, resulting in significant beam wandering that could not be adequately corrected. The soldering iron was held and waved by hand to increase the effect of turbulence, and the individual holding the soldering iron was not informed of the presence or absence of the delay. The standard deviations of beam wandering were 99.0 μm in the x-direction and 39.8 μm in the y-direction when a 0.5-s delay was added, and 13.6 μm and 18.6 μm, respectively, for the phase conjugate light without delay. The results showed that elimination of the phase conjugate mirror delay could reduce beam wandering by 86% in the x-direction and 53% in the y-direction (figure 3).

Next, a pinhole was placed on the observation path divided by PBS 3 at a location corresponding to the position of the spherical mirror. The center of the pinhole was aligned to that of the phase conjugate light. The power of light passing through the pinhole was measured by a power meter. A comparison of the phase conjugate light with and without the 0.5 s delay showed that the intensity fluctuation was reduced by 55% when no delay was added.

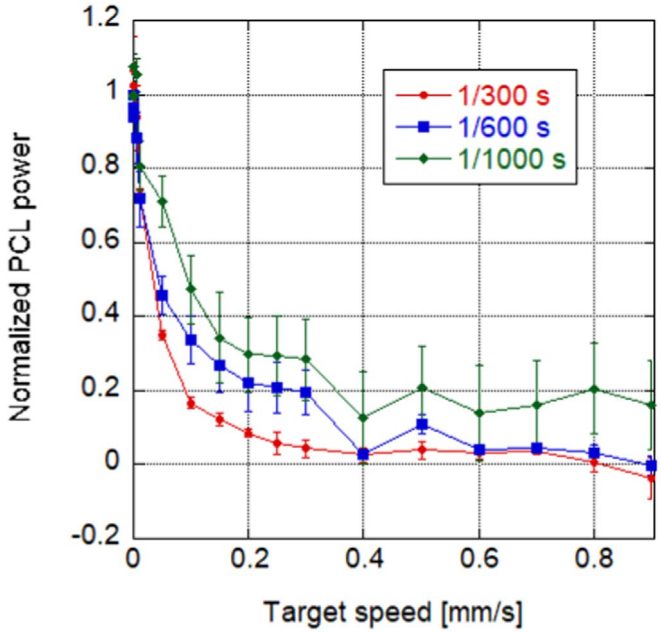

Figure 4. Normalized phase conjugate light output versus the line-of-sight velocity of the target. Solid lines represent a guide to the eye. Shorter exposure time prevents interference fringes from being erased and preserves phase conjugate light output.

Finally, the phase conjugate light was generated while the spherical mirror was continuously moved. When the target was moving, positions of constructive and destructive interference change because of the continuous change of the optical path difference. If the brightness and darkness of the interference fringes were reversed within one exposure time, the interference fringes were averaged, and no phase conjugate light could be generated. Therefore, in actual applications, it is necessary to acquire instantaneous interference fringe patterns using a short-pulse laser. In this study, we used CW light with shutter speeds of 1/300 s, 1/600 s, and 1/1000 s. The output of the phase conjugate light was measured while moving the spherical mirror along the optical axis at a maximum speed of 0.9 mm s^{-1}. At this speed, the brightness and darkness of the interference fringes are reversed approximately six times during a 1 ms exposure. As a result, the power of the phase conjugate light decreased as the moving speed of the target increased, as shown in figure 4, but the power can be maintained by shortening the shutter speed to prevent averaging of interference fringes.

Summary

In this study, a 700 Hz high-speed liquid crystal spatial light modulator and a high-speed camera were used to improve the response time of a digital phase conjugate mirror, achieving a total delay time between signal light acquisition and phase conjugate light generation of 9.7 ms at 1246 × 1024 and 5.9 ms at 640 × 512. The tracking experiment was conducted on a target moving at constant intervals perpendicular to the optical axis, and it was found that the movement of the target and that of the phase conjugate light matched within an error of 2%. In addition, correction experiments for artificially generated air disturbance were conducted using a soldering iron heat source. Compared to the phase conjugate light with an added delay, the phase conjugate light emitted in real time reduced beam wandering by 86% and intensity fluctuation by 55%. In addition, phase conjugate light was emitted to a continuously moving target. Our findings confirmed that a short-pulse laser is necessary to prevent averaging of interference fringes.

In this initial experiment, low-power He-Ne lasers were used to verify the response speed and principle. Taking advantage of the fact that this digital phase conjugate mirror can be used with any laser, we further aim to conduct field tests with higher-energy lasers.

Data availability statement

The data cannot be made publicly available upon publication because they are not available in a format that is sufficiently accessible or reusable by other researchers. The data that support the findings of this study are available upon reasonable request from the authors.

Funding

JSPS KAKENHI Grant Number (JP18K13927); Kitasato University Research Grant for Young Researchers.

Disclosures

The authors declare that there are no conflicts of interest related to this article.

ORCID iDs

Kotomi Kawakami https://orcid.org/0000-0003-2118-5799

References

[1] Summerer L and Purcell O 2009 *Concepts for wireless energy transmission via laser (Leopold & Purcell, Oisin)*
[2] Jin K and Zhou W 2019 Wireless laser power transmission: a review of recent progress, *IEEE Trans. Power Electron.* **34** 3842–59
[3] Weichel H 1990 *Laser Beam Propagation in the Atmosphere* ed R F Potter (Washington: SPIE) ch 5
[4] Murty S S R 1979 Laser beam propagation in atmospheric turbulence *Proc. Indian Acad. Sci. (Engg. Sci.)* 2, 179–195
[5] Kapranov V V, Matsak I S, Yu. Tugaenko V, Blank A V and Suhareva N A 2017 Atmospheric turbulence effects on the performance of the laser wireless power transfer system *Proc. SPIE 10096, Free-Space Laser Communication and Atmospheric Propagation XXIX* 100961E 24 February (https://doi.org/10.1117/12.2252013)
[6] Kawashima N, Takeda K and Yabe K 2007 Application of the laser energy transmission technology to drive a small airplane *Chin. Opt. Lett.* **5** S109–10
[7] Lee S, Alexander J W and Jeganathan M 2000 Pointing and tracking subsystem design for optical communications link between the International Space Station and ground *Proc. SPIE* **3932** 150–7
[8] Guthery C E and Michael H 2021 Pyramid and Shack-Hartmann hybrid wave-front sensor *Opt. Lett.* **46** 5
[9] Bonnefois A M *et al* 2018 Adaptive optics pre-compensation for GEO feeder links: The FEEDELIO experiment *Proc. SPIE 11180, Int. Conf. on Space Optics — ICSO* 111802C
[10] Xiong Y and Feng H 2003 Applications of adaptive optics in lunar laser ranging *Proc. SPIE 4839, Adaptive Optical System Technologies II* **4839** 88–93
[11] He G S 2002 Optical phase conjugation: principles, techniques, and applications *Prog. Quantum Electron.* **26** 131–91
[12] Pepper D M and Yariv A 1980 Compensation for phase distortions in nonlinear media by phase conjugation *Opt. Lett.* **5** 59–60
[13] Fisher R A 1983 *Optical Phase Conjugation* (New York: Academic)
[14] Sakai J 1992 *Phase conjugate optics (advanced science & technology)* (New York: McGraw-Hill)
[15] Cui M and Yang C 2010 Implementation of a digital optical phase conjugation system and its application to study the robustness of turbidity suppression by phase conjugation *Opt. Express* **18** 3444–55
[16] Gigan S *et al* 2021 Roadmap on wavefront shaping and deep imaging in complex media *J. Phys.: Photonics* **4** 042501
[17] Salter P S and Booth M J 2019 Adaptive optics in laser processing *Light: Sci. Appl.* **8** 110
[18] Hillman T R, Yamauchi T, Choi W, Dasari R R, Feld M S, Park Y and Yaqoob Z 2013 Digital optical phase conjugation for delivering two-dimensional images through turbid media *Sci Rep.* **3** 1909
[19] Kawakami K, Uchida S and Okamura H 2014 Real-time compensation of phase distortions by digital phase conjugation using CCD and liquid crystal panel *Appl. Opt.* **53** 3663–7
[20] Sergeyev A V and Roggemann M C 2011 Monitoring the statistics of turbulence: Fried parameter estimation from the wavefront sensor measurements *Appl. Opt.* **50** 3519–28
[21] Wang D, Zhou E H, Brake J, Ruan H, Jang M and Yang C 2015 Focusing through dynamic tissue with millisecond digital optical phase conjugation *Optica.* **2** 728–35
[22] Kumar M, Quan X, Awatsuji Y, Cheng C, Hasebe M, Tamada Y and Matoba O 2020 Common-path multimodal three-dimensional fluorescence and phase imaging system *J. Biomed. Opt.* **25** 032010
[23] Matsusue K, Kishikawa H and Goto N 2020 Experimental demonstration of atmospheric turbulence emulated by soldering iron-induced air convection on orbital angular momentum beam *Opto-Electronics and Communications Conf. (OECC)* (Taipei, Taiwan) (https://doi.org/10.1109/OECC48412.2020.9273589)